Modeling and Design of Passive Components for Flexible Electronics

Nikola Jeranče, Nataša Samardžić, Dragana Vasiljević, and Goran Stojanović

Abstract—In this paper, electromagnetic modeling of capacitors and inductors for printed electronic circuits is studied. Capacitors are successfully modeled by two-dimensional finite element software. Capacitive sensor for chemical detection is proposed and tested in water. Inductors are modeled by the integrating through the currents and obtained results have been compared with 3D finite element method. A capacitive sensor and an inductor on flexible substrate were fabricated. Simulation results have been validated through measurements.

Index Terms—Sensors, Capacitors, Inductors, Printed electronics.

I. INTRODUCTION

ELECTRONICS on flexible substrate is rapidly developing, promising new applications and low-cost components and circuits [1]. Although new applications with active components such as thin film transistors and organic light emitting diodes are very promising, the development of passive components is also important. Design of capacitors and inductors described in this paper is done for two purposes: circuit components needed to achieve desired response in frequency domain and variable capacitors and inductors for sensors application. For example, capacitive sensors can be used as chemical sensors in food intelligent packages [2]. Inductive position sensors are widely used in industrial and automotive applications. Accurate modeling of components in printed flexible circuits is the basis of their efficient design and development. The electromagnetic modeling methods, taking into account the specific properties of printed flexible circuits, are explored.

II. CAPACITORS ON A FLEXIBLE SUBSTRATE

In this paper, capacitors have been modeled in Comsol Multiphysics finite element software package as a classical electrostatics problem. Considered geometries allow us to do the simulations in two dimensions (2D), which is faster and more convenient for electromagnetic design.

A. Selecting the Capacitor Structure

First simulated structures are capacitors in the shape of tube with electrode polarity shown on a cross section in Fig. 1. This figure presents the potential scale going from 0 (blue) to 1 V (red), whereas Fig.1(b)-Fig.1(d) show tube capacitors with different potential distributions obtained by electrodes on the outside wall. The results for capacitance for 20 mm length in third dimension (l) at $\varepsilon_r = 1$, and the change for $\varepsilon_r = 10$ in the tube, are given in Table I.

Another type of structures has been proposed, to fully exploit new possibilities with flexible substrate: spirally rolled capacitors. The electrodes were printed on a substrate

TABLE I
SIMULATION RESULTS FOR FLEXIBLE CAPACITORS

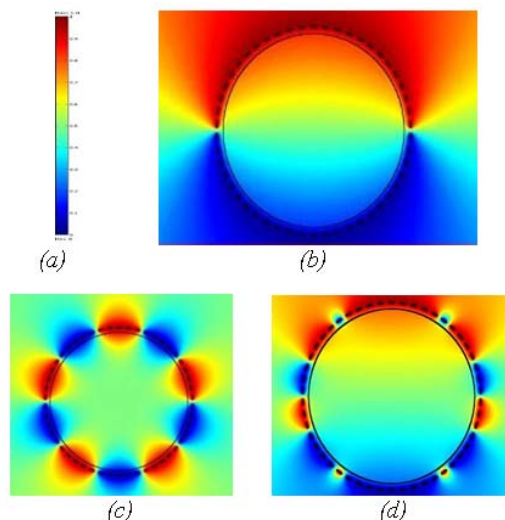| Design shown in figure	Outside diameter (mm)	C_0 (pF) for $\varepsilon_r = 1$ $l = 20$ mm	$\dfrac{\Delta C}{C_0}$ for $\varepsilon_r = 10$	Uniform field
1.(b)	3.2	1.08	128%	no
1.(c)	3.2	3.78	40%	no
1.(d)	3.2	4.08	29%	yes
2.(b)	7	58	900%	yes
2.(c)	9.5	24.2	900%	yes

Fig. 1. Tube-shaped capacitors.

which is wound in a spiral shape so that positive and negative electrodes always come in front of each other.

The shape of substrate cross section is shown in Fig. 2(a) and first designs are shown in Fig. 2(b) and 2(c), whereas capacitance and its relative change are given in Table I.

These results are very encouraging: easily increased capacitance, very high sensitivity (following the change of ε_r) and very uniform electric field in the structure.

B. Spiral Capacitive Sensor – Simulations

To get a spiral shape of structure, at the beginning, an approximation with 8 straight lines per turn has been used. Cross section of that structure is shown in Fig. 3 and the results for capacitance for 10 mm length in third dimension (l), 0.5 mm distance between electrodes, inner diameter 3 mm and external diameter 5 mm at $\varepsilon_r = 1$, and the change for $\varepsilon_r = 10$ in the tube, are given in Table II.

W is electric energy in 2D (per length), and C is capacitance calculated as:

$$C = \frac{2 \cdot W \cdot l}{U^2} \tag{1}$$

U is voltage applied to the electrodes and its value was
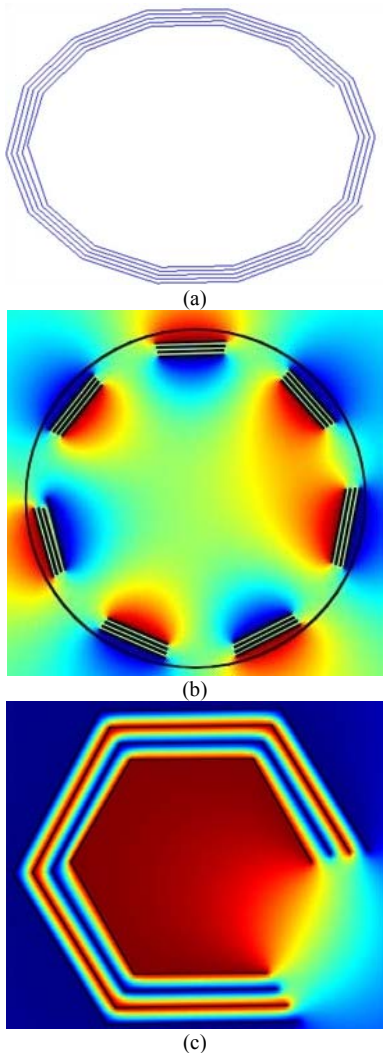

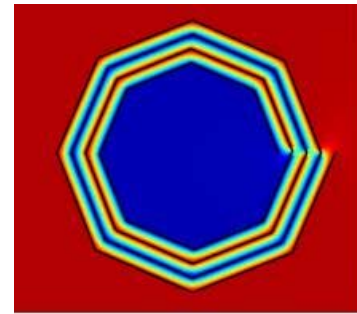(a)

(b)

(c)

Fig. 2. Spirally-shaped capacitors.

Fig. 3. Cross section of a spirally-rolled capacitor with 8 straight lines per turn.

TABLE II
SIMULATION RESULTS FOR CAPACITORS ON A FLEXIBLE SUBSTRATE DUE TO THE CHANGE OF ε_r

ε_r	W [N]	C [pF]
1	1.932751e-9	38.65502
10	1.932751e-8	386.5502

taken as 1 V, to make calculation easier.

After several simulations, for different number of straight lines per turn, it has been found that for more than 12 lines per turn, results do not change significantly, which it can be seen in Table III, therefore this number of straight lines was adopted as final.

The flexible substrate for manufacturing this capacitive sensor has $\varepsilon_r=3$. For practical reasons, to prevent short circuit of the electrodes, gap between electrodes is left, which is shown in Fig. 4. Cross section of this structure and the results with the influence of the dielectric constant of substrate are shown in Fig. 4 and Table IV, respectively.

To make a constant distance between the electrodes we used a paper, which has a dielectric constant $\varepsilon_r=3$. The paper would also allow water to enter between the electrodes and to change ε_r which will be measured. Simulation results for $\varepsilon_r=3$ (ε_r of the paper between the electrodes) and variation for $\varepsilon_r=80$

TABLE III
SIMULATION RESULTS FOR DIFFERENT NUMBER OF STRAIGHT LINES PER TURN (N), FOR $\varepsilon_r = 1$

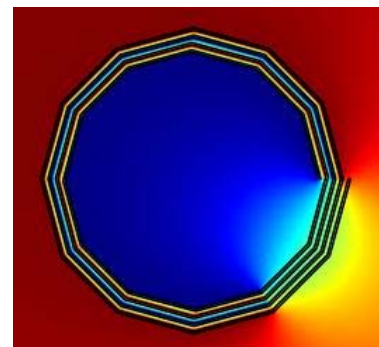| n	W [N]	C [pF]
8	7.021128e-10	14.04226
10	6.891024e-10	13.78205
12	6.836755e-10	13.67351

Fig. 4. Cross section of a spirally rolled capacitor with 12 straight lines per turn.

TABLE IV
SIMULATION RESULTS FOR CAPACITORS ON A FLEXIBLE SUBSTRATE WITH
INFLUENCE OF $\varepsilon_r = 1$

ε_r	W [N]	C [pF]
1	1.725202e-9	34.50404
10	7.461256e-9	149.2251

TABLE V
SIMULATION RESULTS FOR INFLUENCE OF ENVIRONMENT

ε_r	W [N]	C [pF]
3	3.996441e-9	79.92883
80	1.133231e-9	226.6462

TABLE VI
MEASUREMENT RESULTS FOR $\varepsilon_r = 3$, AND ITS CHANGE FOR $\varepsilon_r = 80$

ε_r	C [pF]
3	79.5573
80 (immediately)	217.196
80 (after 24 h)	268.010

(ε_r of water, where sensor would be placed) are given in Table V, for substrate thickness of 50 μm, paper thickness of 100 μm, and inner radius of 2.5 mm.

C. Spiral Capacitive Sensor – Measurements

Simulation results given in Table V have been verified by measuring the structure shown in Fig. 5 using the Impedance/Gain-Phase Analyzer HP4194A.

The first set of measurements presents capacitance variation at different frequencies. The capacitance was measured at five different frequencies and these results are shown in Fig. 6.

Fig. 6 also shows that changes in capacitance as a function of the frequency are very small so they can be neglected (the average value is considered). The next step was to verify how the dielectric constant affects the capacitance. Measurements were performed for two values of dielectric constants between electrodes, for ε_r=3 (the dielectric constant of paper) and for ε_r=80 (the dielectric constant of water). Those results are given in Table VI.

As it can be seen from Table V and VI the results of measurements are in very good agreement with the results obtained through the simulations. The next step was to test how putting Kapton film in water affects the capacitance. This test has been performed using the capacitor with the same design and dimensions as the previous one, but without the
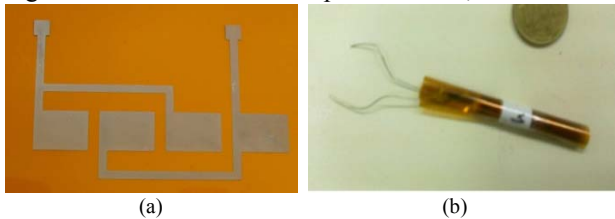

(a)   (b)
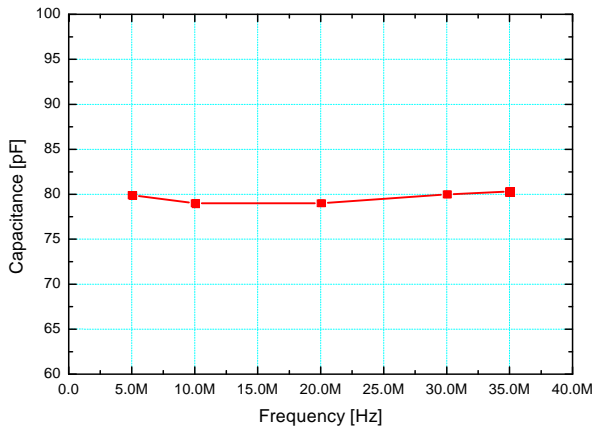Fig. 5. Fabricated capacitive sensor (a) unwrapped and (b) wrapped.

Fig. 6. Measured capacitance at different frequencies.

paper between the electrodes. In the Table VII, measured capacitance results are given, when Kapton film is dry or exposed to the water for 24 h.

Bearing in mind that dielectric constant of water is much greater than dielectric constant of Kapton film, influence of the water layer (absorbed by paper) can be neglected. This can be seen in Table VI and VII. The presented results show that the sensor works properly, allowing measurement of changes in dielectric constant of the environment.

III. INDUCTORS ON A FLEXIBLE SUBSTRATE

Inductors can be modelled in finite element software, as three-dimensional (3D) magnetostatic problem. However, the absence of ferromagnetic materials in modelled circuits has allowed us to simplify the inductance calculation by integrating vector potentials in the circuit. In this manner, there is no need for time and memory consuming 3D finite element computation as well as the problem of domain truncation (which can affect finite element results) is avoided. The in-house developed program for inductance calculation has been validated through comparison with analytical expressions and also with finite element method.

A. Simulations by the Finite Element Method

Inductance calculations were firstly performed in COMSOL Multiphysics finite element software package. Simple conductive segments with rectangular shape were simulated as 3D magnetostatic problem using the method where the model is solved for magnetic potential and calculation has been performed through magnetic energy Wm:

$$L = \frac{2W_m}{I^2} \tag{2}$$

where: L – inductance, I – total current.

Current density is set as input parameter and adjusted so that total current through the structure is equal to 1 A.

The mesh for this type of problem (electronic circuits on flexible substrate) can contain many elements. This is due to

TABLE VII
THE EFFECT OF WATER ABSORBED IN KAPTON FILM ON MEASURED
CAPACITANCE

$\varepsilon_{rKapton}$	C [pF]
dry	207.199
wet (after 24 h)	236.912

thin conductors and a lot of empty space around them which must be included in the model in order to represent the field correctly. In our models, we use thicker conductors, limiting the task to find the correct inductances in such cases, so that we can test our program.

Simulations were run for rectangle structures of different dimensions: 20 mm x 4 mm x 1mm, 10 mm x 1 mm x 1 mm and 10 mm x 2 mm x 0.5 mm (length x width x thickness).

Modeling was improved by using infinite elements: the studied domain is divided into two boxes – the inner box represents local domain and the external box represents infinity domain, thus avoiding huge number of elements, saving memory and time of computation. Default parameters for mapped infinite elements of Cartesian, cylindrical or spherical geometries are available in our software as an option, for the user to optimize calculations problem.

Simulations were run for different distances between box and the structure in Cartesian system and calculations of inductance were performed with energy density. Results were compared with those from analytical expression [4]:

$$L = 0.002 \left\{ \ln \left[\frac{2l}{w+t} \right] + 0.5 + \left(\frac{w+t}{3l} \right) \right\} \quad (3)$$

where w and t are dimensions of cross section, l stands for length of conductive segment in centimeters.

The best agreement has been obtained for inner box of 15 mm distance of every structure edge and 20 mm distance for larger box.

The same structures were calculated using our in-house developed program written in C++. The obtained values of inductances by analytical expressions, COMSOL and C++ simulations are given in the Table VIII.

After that, COMSOL Multiphysics was used for simulating spiral shaped inductor structure with initial radius of 3 mm which is increased for 0.5 mm at each full turn. Simulated structure corresponds to a half of one turn. Cylinders were used as boundaries for defining infinite elements. The simulation results for spirally rolled conductor obtained in COMSOL and by our program are given in Table IX.

B. Simulations by the Integrating

A computer program is written in C++ which calculates all inductances in a circuit. An inductor consists of straight conductive segments which can be printed on flexible substrate. Each straight segment is divided into small volume elements.

The inductance is calculated by integrating over the elements using the formula [3]:

$$L = \frac{1}{I^2} \int \vec{J} \, \vec{A} \, dv \quad (4)$$

where: $\vec{J}$ – current density vector in the element; $\vec{A}$ – vector potential at the center of element; dv – volume of the element. The vector potential at a point is computed by the formula [3]:

$$A = \frac{\mu}{4\pi} \int \frac{\vec{J}}{R} \, dv \quad (5)$$

TABLE VIII
RESULTS OF SIMULATION FOR RECTANGLE INDUCTANCE

Rectangle dimension (mm)	Analytical inductance value (nH)	COMSOL's inductance (nH)	C++ inductance (nH)
20 x 4 x 1	10.653	10.642	10.875
10 x 1 x 1	5.744	5.249	5.768
10 x 2 x 0.5	5.326	5.317	5.438

TABLE IX
SIMULATED ROLLED INDUCTANCE RESULTS

Software tool	Inductance, L (nH)
COMSOL	3.847
C++	4.03

where: R – distance to the point where $\vec{A}$ is computed; μ – magnetic permeability.

The end point coordinates of the straight segments are entered in u-v plane, thus giving the initial coordinates and direction of (assumed to be parallel with the segment: a correct approximation if the segment is long enough) and vector normal to the surface for each element. These coordinates and vector directions are transformed into x-y-z Cartesian coordinate system by using appropriate mathematical expression to correspond to the shape of the twisted flexible substrate. In this manner, we avoid drawing complicated geometries in three dimensions and the component is described in the same way as it is fabricated afterwards. All self inductances and mutual inductances of individual segments and conductors are available in an output file, in order to make verification and circuit design easier.

In-house developed program has been tested for straight line segments (no twisting), circular conductors and spirally rolled conductors, which corresponds to the existing separate parts of the program code.

The results have been validated in three ways: through comparison with analytical expressions for self and mutual inductances where this was possible, through comparison with finite element results and, finally, through measurements.

A meander-shaped inductor shown in Fig. 7(a), were printed on a flexible substrate which is then wound into spiral shape to obtain the conductor geometry shown in Fig. 7(b). The spiral starts at radius 5 mm and 0.075 mm is added at each full turn, the vertical line segments are 10 mm long, all straight segments are 2 mm wide, 10 μm thick. For the inductor in the plane we obtain the total inductance of 202 nH. For an illustration, self inductance of a straight 10 mm long segment obtained by the in-house developed program is 5.75 nH, while the value obtained by analytical expression (3) is 5.74 nH.

Total inductance of spirally rolled inductor calculated by our program is 514 nH.

We can simply test the part of the code describing circular conductors by calculating the inductance of a solenoid made of straight conductor printed on a flexible substrate and then wound around an axis. Line width is now the height of the solenoid and its length is equal to solenoid's circumference. For height equal to 100 mm and radius of 10 mm, the program calculates 4.06 nH inductance, compared to 3.95 nH obtained
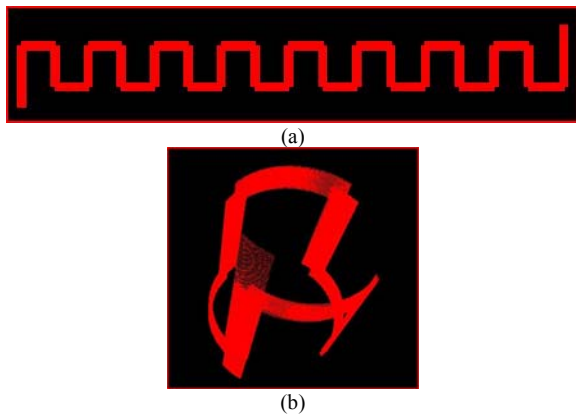
(a)

(b)

Fig. 7. (a) Meander inductor and (b) the spirally rolled inductor obtained by winding.

by well-known formula [4] for long solenoid.

Comparison with COMSOL finite element package has been done for straight rectangular segments (see Table VIII) and for spiral inductor for which the results are given in Table IX. Good agreement between finite element method and in-house developed program allows us to apply the program for more complex simulations and to adjust it to the needs of flexible circuit simulations.

C. Spirally Rolled Inductor – Measurements

In order to validate our simulation results, meander inductor in the plane and rolled were fabricated using ink-jet printing technology. The printed meander structure is the one presented in Fig. 7, with straight segments 2 mm wide, 10 mm length of vertical linear segments, while the rolled structure has 5 mm inner radius. The printing were done on Kapton film substrate with silver nanoparticle ink, using Dimatix DMP-3000 inkjet printer [5]. Thickness of the used substrate is 75 μm. Fig. 8 shows fabricated structure.

Measurements were performed with Impedance Analyzer HP4194A both for unwrapped and wrapped inductor. Inner radius of wrapping was 5 mm. The fabricated rolled meander inductor is shown in Fig. 9.

The simulation by the C++ program has given 202 nH for unwrapped and 514 nH as the inductance for the wrapped structure. It is known from simulation results that inductance value was around few hundreds of nH, thus we could conclude that copper wires' inductance used to connect testing component with Analyzer cannot be neglected. For that reason we measured wires' influence first and then subtracted those values from the total measured inductance to obtain the accurate inductance of the rolled structure.

Graphs from Fig. 10 represent changes of inductance as a function of frequency for unwrapped and wrapped meander

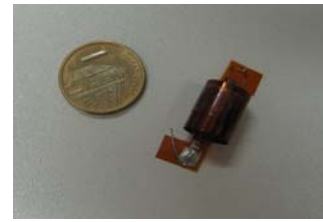Fig. 8. Meander inductor on flexible Kapton substrate.

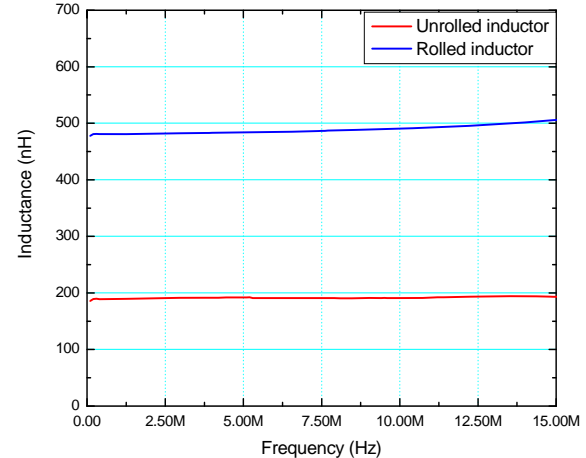Fig. 9. The rolled meander inductor structure.

Fig. 10. Measured results of meander inductance for straight segments (red down line) and for wrapped structure (blue upper line).

inductor structure. Average value of total inductance in the first case is 190 nH and for wrapped case is 490 nH. As it can be seen, graphs showed a good agreement with simulated results.

IV. CONCLUSION

Modeling and design of capacitors and inductors printed on flexible substrates has been studied. Simulations of capacitive structures were done by 2D finite element software. Spiral sensor structures have been successfully simulated and a chemical sensor with high sensitivity has been designed. The sensor design has been validated through measurements. The time-consuming 3D finite element simulations of inductive structures were avoided by integrating vector potentials due to currents. The accuracy of the in-house developed program has been validated by comparison with analytical results, finite element results and measurements. The agreement of the obtained results is very good.

REFERENCES

[1]   Frances Gardiner, Eleanor Carter, "Polymer electronics – a flexible technology", iSmithers, 2009.

[2]   Mohd Syaifudin Bin Abdul Rahman, Subhas C. Mukhopadhyay, Pak Lam Yu, "Novel Sensors for Food Inspections", Sensors & Transducers Journal, Vol. 114, Issue 3, March 2010, pp. 1-40.

[3]   W.R. Smythe, "Static and dynamic electricity", 1950, McGraw-Hill Book Company.

[4]   H. Greenhouse, "Design of planar rectangular microelectronic inductors", IEEE Trans. Parts Hybrids, Packaging, Vol. PHP-10, pp.101-109.

[5]   www.dimatix.com.